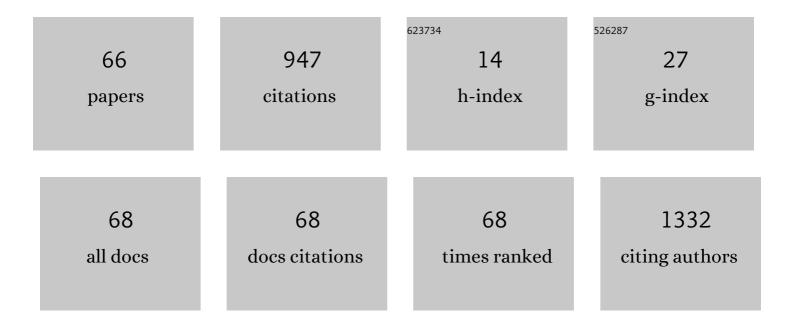
List of Publications by Year in descending order

Source: https://exaly.com/author-pdf/7901251/publications.pdf Version: 2024-02-01



#	Article	IF	CITATIONS
1	Prognostic Significance of Dynamic ¹⁸ F-FET PET in Newly Diagnosed Astrocytic High-Grade Glioma. Journal of Nuclear Medicine, 2015, 56, 9-15.	5.0	144
2	First Clinical Results for PSMA-Targeted α-Therapy Using ²²⁵ Ac-PSMA-I&T in Advanced-mCRPC Patients. Journal of Nuclear Medicine, 2021, 62, 669-674.	5.0	87
3	Predictive Value of ^{99m} Tc-MAA SPECT for ⁹⁰ Y-Labeled Resin Microsphere Distribution in Radioembolization of Primary and Secondary Hepatic Tumors. Journal of Nuclear Medicine, 2015, 56, 1654-1660.	5.0	74
4	Safety, Efficacy, and Prognostic Factors After Radioembolization of Hepatic Metastases from Breast Cancer: A Large Single-Center Experience in 81 Patients. Journal of Nuclear Medicine, 2016, 57, 517-523.	5.0	48
5	PET Response Criteria in Solid Tumors Predicts Progression-Free Survival and Time to Local or Distant Progression After Chemotherapy with Regional Hyperthermia for Soft-Tissue Sarcoma. Journal of Nuclear Medicine, 2015, 56, 530-537.	5.0	31
6	Positron emission tomography based in-vivo imaging of early phase stem cell retention after intramyocardial delivery in the mouse model. European Journal of Nuclear Medicine and Molecular Imaging, 2013, 40, 1730-1738.	6.4	29
7	Coupling between physiological TSPO expression in brain and myocardium allows stabilization of late-phase cerebral [18F]GE180 PET quantification. NeuroImage, 2018, 165, 83-91.	4.2	27
8	Left ventricular functional assessment in murine models of ischemic and dilated cardiomyopathy using [18 F]FDG-PET: comparison with cardiac MRI and monitoring erythropoietin therapy. EJNMMI Research, 2012, 2, 43.	2.5	21
9	3D Monte Carlo bone marrow dosimetry for Lu-177-PSMA therapy with guidance of non-invasive 3D localization of active bone marrow via Tc-99m-anti-granulocyte antibody SPECT/CT. EJNMMI Research, 2019, 9, 76.	2.5	21
10	FDG-PET reveals improved cardiac regeneration and attenuated adverse remodelling following Sitagliptin + G-CSF therapy after acute myocardial infarction. European Heart Journal Cardiovascular Imaging, 2016, 17, 136-145.	1.2	20
11	[68Ga]-Albumin-PET in the Monitoring of Left Ventricular Function in Murine Models of Ischemic and Dilated Cardiomyopathy: Comparison with Cardiac MRI. Molecular Imaging and Biology, 2013, 15, 441-449.	2.6	19
12	Patient-specific image-based bone marrow dosimetry in Lu-177-[DOTA0,Tyr3]-Octreotate and Lu-177-DKFZ-PSMA-617 therapy: investigation of a new hybrid image approach. EJNMMI Research, 2018, 8, 76.	2.5	19
13	Outcome and Safety after 103 Radioembolizations with Yttrium-90 Resin Microspheres in 73 Patients with Unresectable Intrahepatic Cholangiocarcinoma—An Evaluation of Predictors. Cancers, 2021, 13, 5399.	3.7	17
14	Response to 225Ac-PSMA-I&T after failure of long-term 177Lu-PSMA RLT in mCRPC. European Journal of Nuclear Medicine and Molecular Imaging, 2021, 48, 1262-1263.	6.4	16
15	Positron emission tomography in the assessment of left ventricular function in healthy rats: A comparison of four imaging methods. Journal of Nuclear Cardiology, 2013, 20, 262-274.	2.1	15
16	3D image-based dosimetry for Yttrium-90 radioembolization of hepatocellular carcinoma: Impact of imaging method on absorbed dose estimates. Physica Medica, 2020, 80, 317-326.	0.7	15
17	18F-FDC-PET/CT in Patients with Advanced, Radioiodine Refractory Thyroid Cancer Treated with Lenvatinib. Cancers, 2021, 13, 317.	3.7	15
18	Dosimetry and optimal scan time of [18F]SiTATE-PET/CT in patients with neuroendocrine tumours. European Journal of Nuclear Medicine and Molecular Imaging, 2021, 48, 3571-3581.	6.4	15

#	Article	IF	CITATIONS
19	68Ga-EMP-100 PET/CT—a novel ligand for visualizing c-MET expression in metastatic renal cell carcinoma—first in-human biodistribution and imaging results. European Journal of Nuclear Medicine and Molecular Imaging, 2022, 49, 1711-1720.	6.4	15
20	Long-term outcome of rare oncocytic papillary (Hürthle cell) thyroid carcinoma following (adjuvant) initial radioiodine therapy. European Journal of Nuclear Medicine and Molecular Imaging, 2019, 46, 2526-2535.	6.4	14
21	Clinical impact of follicular oncocytic (Hürthle cell) carcinoma in comparison with corresponding classical follicular thyroid carcinoma. European Journal of Nuclear Medicine and Molecular Imaging, 2021, 48, 449-460.	6.4	14
22	Cost-Effectiveness Analysis of 68Ga DOTA-TATE PET/CT, 111In-Pentetreotide SPECT/CT and CT for Diagnostic Workup of Neuroendocrine Tumors. Diagnostics, 2021, 11, 334.	2.6	14
23	Influence of dosimetry method on bone lesion absorbed dose estimates in PSMA therapy: application to mCRPC patients receiving Lu-177-PSMA-I&T. EJNMMI Physics, 2021, 8, 26.	2.7	13
24	Temporal Changes in Phosphatidylserine Expression and Glucose Metabolism after Myocardial Infarction: An in Vivo Imaging Study in Mice. Molecular Imaging, 2012, 11, 7290.2012.00010.	1.4	12
25	Erroneous cardiac ECG-gated PET list-mode trigger events can be retrospectively identified and replaced by an offline reprocessing approach: first results in rodents. Physics in Medicine and Biology, 2013, 58, 7937-7959.	3.0	12
26	In-vivo monitoring of erythropoietin treatment after myocardial infarction in mice with [68Ga]Annexin A5 and [18F]FDG PET. Journal of Nuclear Cardiology, 2014, 21, 1191-1199.	2.1	12
27	124I-PET Assessment of Human Sodium Iodide Symporter Reporter Gene Activity for Highly Sensitive In Vivo Monitoring of Teratoma Formation in Mice. Molecular Imaging and Biology, 2015, 17, 874-883.	2.6	12
28	Feasibility of [68Ga]Ga-FAPI-46 PET/CT for detection of nodal and hematogenous spread in high-grade urothelial carcinoma. European Journal of Nuclear Medicine and Molecular Imaging, 2022, 49, 3571-3580.	6.4	12
29	Noninvasive image derived heart input function for CMRglc measurements in small animal slow infusion FDG PET studies. Physics in Medicine and Biology, 2012, 57, 8041-8059.	3.0	11
30	In Vivo Monitoring of Parathyroid Hormone Treatment after Myocardial Infarction in Mice with [⁶⁸ Ga]Annexin A5 and [¹⁸ F]Fluorodeoxyglucose Positron Emission Tomography. Molecular Imaging, 2014, 13, 7290.2014.00035.	1.4	11
31	Real world efficacy and safety of multi-tyrosine kinase inhibitors in radioiodine refractory thyroid cancer. Thyroid, 2021, 31, 1531-1541.	4.5	11
32	Nephroprotective effects of enalapril after [177Lu]-DOTATATE therapy using serial renal scintigraphies in a murine model of radiation-induced nephropathy. EJNMMI Research, 2016, 6, 64.	2.5	10
33	Monitoring of Cardiac Remodeling in a Mouse Model of Pressure-Overload Left Ventricular Hypertrophy with [18F]FDG MicroPET. Molecular Imaging and Biology, 2018, 20, 268-274.	2.6	10
34	The added diagnostic value of complementary gadoxetic acid-enhanced MRI to 18F-DOPA-PET/CT for liver staging in medullary thyroid carcinoma. Cancer Imaging, 2019, 19, 73.	2.8	10
35	Correlation of an Index-Lesion-Based SPECT Dosimetry Method with Mean Tumor Dose and Clinical Outcome after 177Lu-PSMA-617 Radioligand Therapy. Diagnostics, 2021, 11, 428.	2.6	10
36	Assessment of right ventricular sympathetic dysfunction in patients with arrhythmogenic right ventricular cardiomyopathy: An 123I-metaiodobenzylguanidine SPECT/CT study. Journal of Nuclear Cardiology, 2020, 27, 2402-2409.	2.1	8

#	Article	IF	CITATIONS
37	Effects of the Minimal Extrathyroidal Extension on Early Response Rates after (Adjuvant) Initial Radioactive Iodine Therapy in PTC Patients. Cancers, 2020, 12, 3357.	3.7	8
38	18F–FDG-PET/CT and diffusion-weighted MRI for monitoring a BRAF and CDK 4/6 inhibitor combination therapy in a murine model of human melanoma. Cancer Imaging, 2018, 18, 2.	2.8	7
39	Follow-Up 18F-FDG PET/CT versus Contrast-Enhanced CT after Ablation of Liver Metastases of Colorectal Carcinoma—A Cost-Effectiveness Analysis. Cancers, 2020, 12, 2432.	3.7	7
40	The diagnostic challenge of coexistent sarcoidosis and thyroid cancer – a retrospective study. BMC Cancer, 2021, 21, 139.	2.6	7
41	Impact of Pharmaceutical Prophylaxis on Radiation-Induced Liver Disease Following Radioembolization. Cancers, 2021, 13, 1992.	3.7	7
42	Feasibility of Different Tumor Delineation Approaches for 18F-PSMA-1007 PET/CT Imaging in Prostate Cancer Patients. Frontiers in Oncology, 2021, 11, 663631.	2.8	7
43	Molecular imaging of cardiac CXCR4 expression in a mouse model of acute myocardial infarction using a novel 68Ga-mCXCL12 PET tracer. Journal of Nuclear Cardiology, 2021, 28, 2965-2975.	2.1	6
44	Toxicity of a combined therapy using the mTOR-inhibitor everolimus and PRRT with [177Lu]Lu-DOTA-TATE in Lewis rats. EJNMMI Research, 2020, 10, 41.	2.5	6
45	Temporal changes in phosphatidylserine expression and glucose metabolism after myocardial infarction: an in vivo imaging study in mice. Molecular Imaging, 2012, 11, 461-70.	1.4	6
46	Total Tumor Volume on 18F-PSMA-1007 PET as Additional Imaging Biomarker in mCRPC Patients Undergoing PSMA-Targeted Alpha Therapy with 225Ac-PSMA-1&T. Biomedicines, 2022, 10, 946.	3.2	6
47	Data on specificity of [18F]GE180 uptake for TSPO expression in rodent brain and myocardium. Data in Brief, 2018, 19, 331-336.	1.0	4
48	Incidental Finding of a PSMA-Positive Pancreatic Cancer in a Patient Suffering from a Metastasized PSMA-Positive Prostate Cancer. Diagnostics, 2021, 11, 129.	2.6	4
49	Derivation of a respiration trigger signal in small animal list-mode PET based on respiration-induced variations of the ECG signal. Journal of Nuclear Cardiology, 2016, 23, 73-83.	2.1	3
50	Comparison of metabolic and functional parameters using cardiac 18F-FDG-PET in early to mid-adulthood male and female mice. EJNMMI Research, 2021, 11, 7.	2.5	3
51	Cardiac 18F-FDG Positron Emission Tomography: An Accurate Tool to Monitor In vivo Metabolic and Functional Alterations in Murine Myocardial Infarction. Frontiers in Cardiovascular Medicine, 2021, 8, 656742.	2.4	3
52	Comparison of transient and permanent LAD ligation in mice using 18F-FDG PET imaging. Annals of Nuclear Medicine, 2022, 36, 533-543.	2.2	3
53	Evaluation of Visualization Using a 50/50 (Contrast Media/Glucose 5% Solution) Technique for Radioembolization as an Alternative to a Standard Sandwich Technique. CardioVascular and Interventional Radiology, 2017, 40, 1740-1747.	2.0	2
54	Left-ventricular innervation assessed by 123I-SPECT/CT is associated with cardiac events in inherited arrhythmia syndromes. International Journal of Cardiology, 2020, 312, 129-135.	1.7	2

#	Article	IF	CITATIONS
55	Quantitative myocardial perfusion SPECT/CT for the assessment of myocardial tracer uptake in patients with three-vessel coronary artery disease: Initial experiences and results. Journal of Nuclear Cardiology, 2022, 29, 2511-2520.	2.1	2
56	[68Ca]DOTA-TATE PET for the detection of early transplant rejection in a heterotopic allograft heart transplantation model of the rat: a pilot study. Quarterly Journal of Nuclear Medicine and Molecular Imaging, 2023, 67, .	0.7	2
57	Course of Disease and Clinical Management of Patients with Poorly Differentiated Thyroid Carcinoma. Cancers, 2021, 13, 5309.	3.7	2
58	Detection of cardiac apoptosis by [18F]ML-10 in a mouse model of permanent LAD ligation. Molecular Imaging and Biology, 2022, , 1.	2.6	2
59	Liver Function Changes After Technetium-99m-Macroaggregated Albumin Administration and Their Predictive Value Regarding Hepatotoxicity in Patients Undergoing Yttrium-90-Radioembolization. Anticancer Research, 2021, 41, 437-444.	1.1	1
60	The assessment of left ventricular mechanical dyssynchrony from gated 99mTc-tetrofosmin SPECT and gated 18F-FDG PET by QGS: a comparative study. Journal of Nuclear Cardiology, 2022, 29, 2350-2360.	2.1	1
61	Preoperative Imaging with [18F]-Fluorocholine PET/CT in Primary Hyperparathyroidism. Journal of Clinical Medicine, 2022, 11, 2944.	2.4	1
62	Integrin-targeted quantitative optoacoustic imaging with MRI correlation for monitoring a BRAF/MEK inhibitor combination therapy in a murine model of human melanoma. PLoS ONE, 2018, 13, e0204930.	2.5	0
63	Reply to: "Toxicity and dosimetry in SORAMIC study― Journal of Hepatology, 2020, 73, 735-736.	3.7	0
64	Initial Evaluation of Therapy Response after Adjuvant Radioiodine Therapy in Patients with Early-Stage Papillary Thyroid Cancer—Does Time Matter?. Cancers, 2022, 14, 501.	3.7	0
65	Assessment of left ventricular function with gated myocardial perfusion SPECT and gated myocardial FDG PET in patients with left ventricular mechanical dyssynchrony. Quarterly Journal of Nuclear Medicine and Molecular Imaging, 2021, , .	0.7	0
66	Modulation of Rxrα Expression in Mononuclear Phagocytes Impacts on Cardiac Remodeling after Ischemia-Reperfusion Injury. Biomedicines, 2022, 10, 1274.	3.2	0